

Amalgamation Performance Analysis of LCI and VSI fed Induction Motor Drive

Dilip Kumar¹, Dinesh Kumar², A. K. Srivastava³,

¹Dilip Kumar is Assistant professor of Electrical & Electronics Engineering, Saroj Educational Group Lucknow, U.P, India

²Dinesh Kumar is Assistant Professor of Electrical & Electronic Engineering, KNIT, Sultanpur, U.P,India

³A. K. Srivastava is Assistant Professor of Electrical & Electronic Engineering, KNIT, Sultanpur, U.P,India

Abstract—In this paper combination of a load-commutated inverter (LCI) and a voltage-source inverter (VSI) are employed for performance analysis of induction motor drive. Performance of the drive has been evaluated through the different variation in reference speed and load torque. proposed LCI-based induction motor drives include the following Advantages: 1) sinusoidal motor phase current and voltage based on the instantaneous motor speed control; 2) fast dynamic response by the VSI operation; and 3) elimination of motor torque pulsation. LCI system improves the quality of output current and voltage waveforms and provides the faster dynamic responses. Matlab/Simulation results show the validity of the employed drive system.

Index Terms- Diode rectifier, Induction motor, Load commutated inverter (LCI), SVPWM technique, Voltage source inverter (VSI).

I. INTRODUCTION

The squirrel cage induction motor is basically a simple, less costly and reliable drive and can provide excellent characteristics at a constant shaft speed. Voltage source inverter fed induction motor drives are probably the cheapest and most reliable scheme of speed control [1]. The voltage source inverter fed Induction motor drives most commonly controlled through the pulse width-modulation technique. The voltage source inverter ensures simple and effective motor control since the power circuit can be operated over wide ranges of load frequency and voltage [2]. Yet, the VSI, based on fast-switching insulated-gate bipolar transistors (IGBTs), has shown an intrinsic weakness for high-power applications due to substantial switching losses and high of the pulse width-modulation (PWM) operation, leading to hazardous

over voltages[3]-[4]. Load-commutated inverter (LCI)-based induction motor drives have been used in high-power applications, because of an economical and reliable current source inverter using IGBT-diode and the rugged induction motors [5]. The LCI-based drive employs converter grade thyristors and utilizes soft switching by natural commutation of the IGBT-diode. Therefore, it provides simplicity, robustness, cost effectiveness, and very low switching losses, resulting in a favorable topology in high-power areas [6]- [8]. Moreover, has the current-source inverter (CSI) topology, it has inherent advantages of CSI, such as embedded short-circuit protection, improved converter reliability, and instantaneous regeneration ability [9]. Due to all of these features the LCI-based induction motor drive improves its performance, especially in medium-to-high-power applications [10]. The schematic circuit diagram of the LCI and VSI fed induction motor drive as shown below in Fig.1.

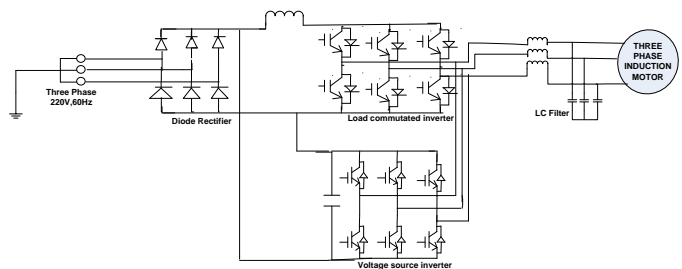


Fig.1 Basic circuit configuration of LCI and VSI fed induction motor drive.

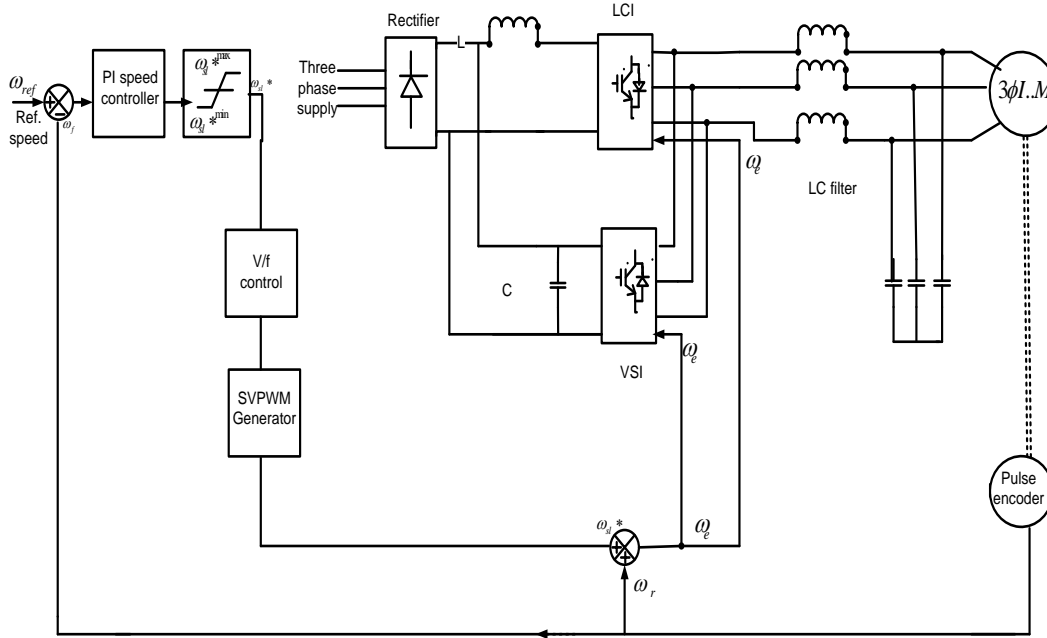


Fig.2. Schematic circuit diagram of LCI and VSI fed induction motor drive.

II. SYSTEM DESCRIPTION

The proposed drive system consisting of a diode rectifier, an LCI, a VSI, an LC filter and three phase induction motor are shown in Fig. 1. The VSI is connected with the LCI in parallel through capacitor DC link. LCI and VSI energized through the same DC link output but the different element. A large inductor DC link is employed for the load commutated inverter. LCI, in order to convert uncontrolled DC voltage to controlled DC current. The DC-link current regulated by the inductor is supplied to the LCI. As a result, both the VSI and the LCI can be fed from the single-diode rectifier. The VSI generates sinusoidal phase voltage to the induction motor. The amplitude and frequency of the VSI output voltage is continuously regulated by the motor speed control. In addition, the phase angle of the VSI output voltage is set from adjusting the firing angle of the LCI to provide a safe LCI commutation angle. Therefore, the leading power factor for the LCI operation is entirely obtained by the VSI over the whole speed range of the induction motor. Based on the leading power factor by the VSI, the presented system can operate the LCI without the dc-commutation circuit as well as output capacitors.

Therefore, the employed system can successfully solve all problems caused by the output capacitors and the forced dc-commutation circuit of the conventional LCI-based induction motor. Another advantage by bringing the VSI is to generate sinusoidal motor currents for all speed regions to large induction motor drives. The parallel assembly of the LCI and the relatively small-size VSI is expected to fulfill the high-power applications, where a stand-alone VSI cannot be utilized to generate sinusoidal motor currents. In addition, the sinusoidal motor voltages are also achieved through the LC filter.

III. CONTROL STRATEGY

A controlled block diagram of the LCI and VSI fed induction motor drive is shown in Fig. 3. It is composed of a three-phase diode rectifier, a load commutated inverter followed by a DC-link inductor, and a three-phase voltage source inverter. The voltage source inverter is connected with the load commutated inverter in parallel. Basically, the proposed system has a combined inverter topology of a load commutated inverter and a voltage source inverter. The load commutated inverter operates in the square-wave mode with converter-grade thyristors. Consequently IGBT-diode in the load commutated inverter turn on and off only once per cycle of the output current and their switching loss is negligible.

The main function of the voltage source inverter is injecting sinusoidal phase voltages to the induction motor. The proposed scheme can generate sinusoidal motor voltages and currents, leading to a reduction in the low-order harmonics injected into the motor. The output power distribution between them, given a certain motor power requirement, is important. A rating factor η is defined as the ratio of the load commutated inverter rating and the voltage source inverter rating. Note that two inverters are connected with the same motor phase voltage in their output terminals; by assuming that voltage drop due to the

Output LC filter for the VSI is negligible. Therefore, the rating factor is directly proportional to the ratio of rms values of the VSI output current and the LCI output current.

$$\eta = \frac{S_{VSI}}{S_{LCI}} = \frac{I_{VSI.rms}}{I_{LCI.rms}} \quad (1)$$

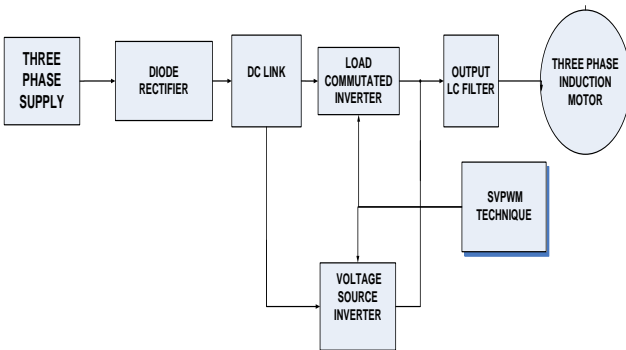


Fig.3 Control block diagram of LCI and VSI fed induction motor drive.

Large power voltage source inverter required for the drive results in a very high system cost. Which will limit the proposed system? From cost point of view, the load commutated inverter is not comparable to the voltage source inverter. Since the motor currents are sinusoidal quantities and the load commutated inverter currents have no ripple components in the dc link, the LCI output current and the motor output current are expressed by:

$$I_o(\omega t) = I_{mo} \cos(\omega t + (\phi + \theta)) \quad (2)$$

The rating factor can be derived, using (1) and (2), by

$$\eta = \sqrt{1 - \frac{3I_{mo}}{I_{dc}} \left\{ \frac{\sqrt{3}}{\pi} (\cos\phi + \theta) - \frac{I_{mo}}{4I_{dc}} \right\}} \quad (3)$$

In addition, is the lagging power factor angle of the induction motor, which is detectable. Then, the dc link current value which minimizes the voltage source inverter rating can be obtained by setting the derivative of η with respect to the dc link current to zero,

$$\frac{d\eta}{dI_{dc}} = 0 \quad (4)$$

This yields an dc link current command I_{dc}^* given by:

$$I_{dc} = \frac{I_{mo}}{2\sqrt{3/\pi}} \cos(\phi + \theta) \quad (5)$$

Equation (5) allows the dc link current control to achieve the minimum voltage source inverter power based on the motor current and phase shift between the motor current and the LCI output current. This dc link current control algorithm is implemented by the dc link inductor.

IV. PERFORMANCE INVESTIGATION OF THE DRIVE

The circuit model is developed to examine the amalgamation performance of the LCI and VSI fed induction motor drive as shown in Fig.2. A three-phase squirrel-cage induction motor rated 3 hp, 220 V, 60 Hz, 1725 rpm is fed by a load commutated inverter and voltage source inverter. The firing pulses to the inverter are generated by the SVPWM modulator block of the SPS library. The chopping frequency is set to 6000 Hz and the input reference vector to magnitude-angle. Speed control of the motor is performed by the constant V/Hz block. The magnitude and frequency of the stator voltages are governed by the speed set point. By varying the stator voltage magnitude in proportion with frequency, the stator flux is kept constant. The performance of the drive is investigated for the following loading conditions:

- Case 1: Starting (0-500rpm)
- Case 2: Speed acceleration (500 rpm - 1000rpm)
- Case 3: Speed acceleration (1000 rpm -1400rpm)
- Case 4: Speed acceleration (1400 rpm -1725rpm)
- Case 5: Speed deceleration (1725 rpm -1400rpm)
- Case 6: Speed deceleration (1400 rpm -1000rpm)
- Case 7: Speed deceleration (1000 rpm -500rpm)
- Case 8: Deceleration in load torque (11.9N-m - 0N-m)
- Case 9: Acceleration in load torque (0N-m -18N-m)
- Case 10: Deceleration in load torque (18N-m - 8N-m)
- Case 11: Acceleration in load torque (8N-m - 11.9N-m)

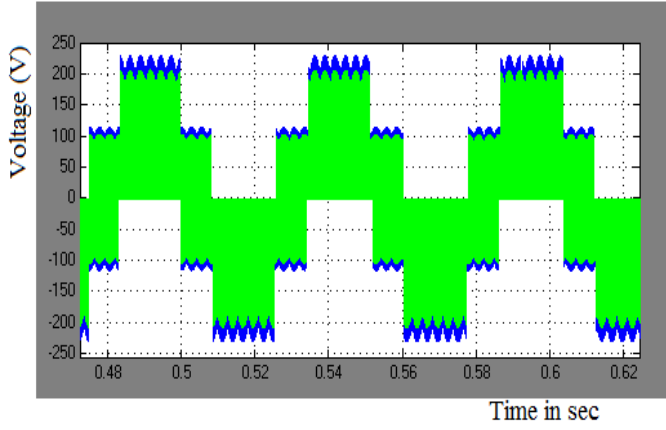


Fig 4.LCI output (V)



Fig. 6. Speed response of the drive for entire performance of rotor speed

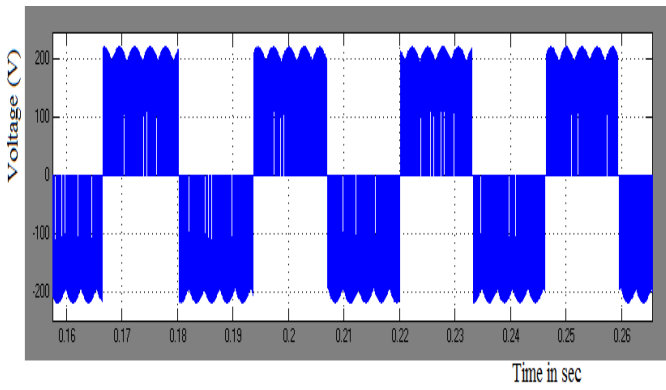


Fig 5.VSI output (V)

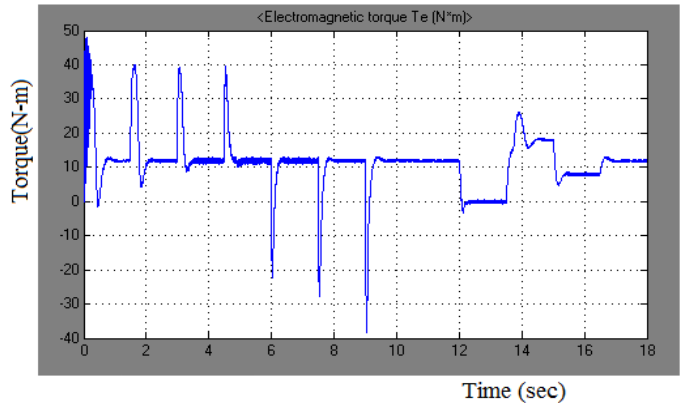
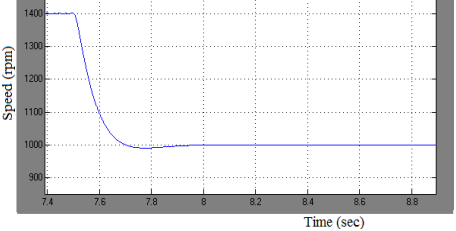
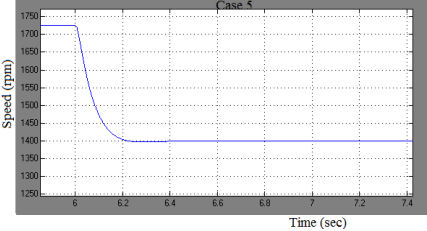
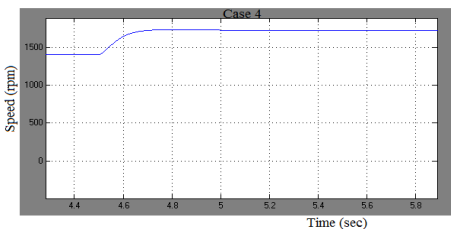
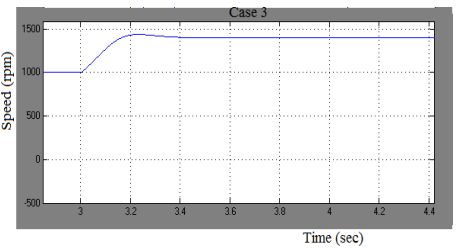
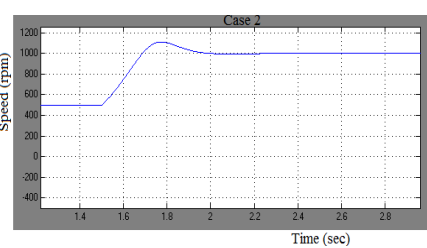
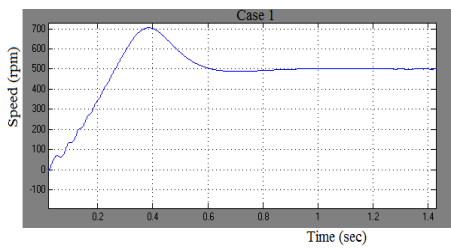


Fig. 7. Torque response of the drive for entire performance of load torque



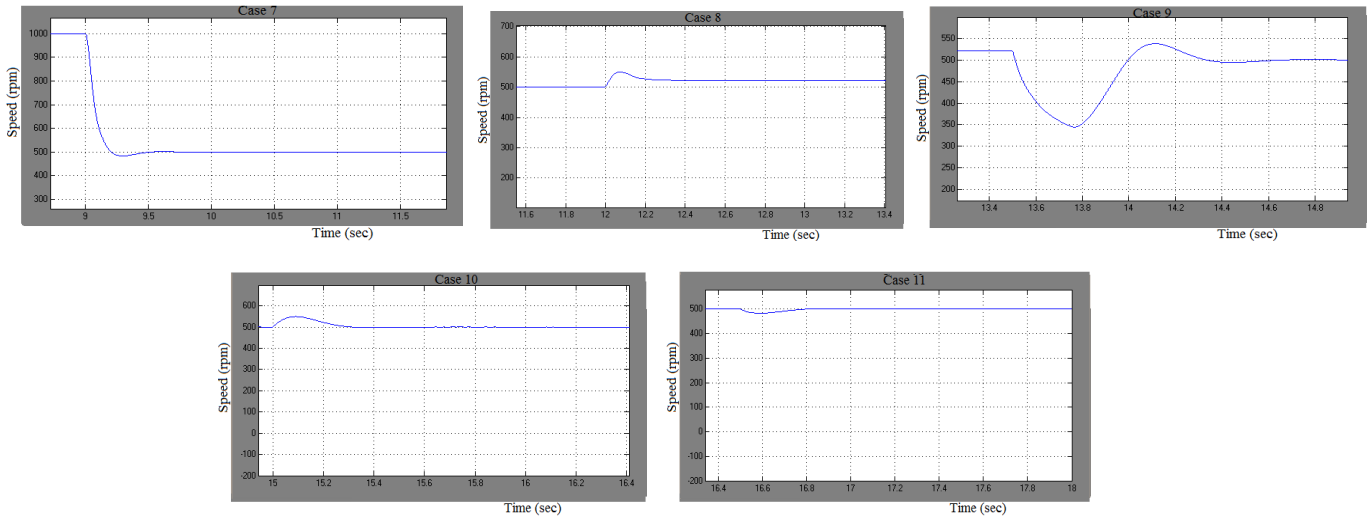
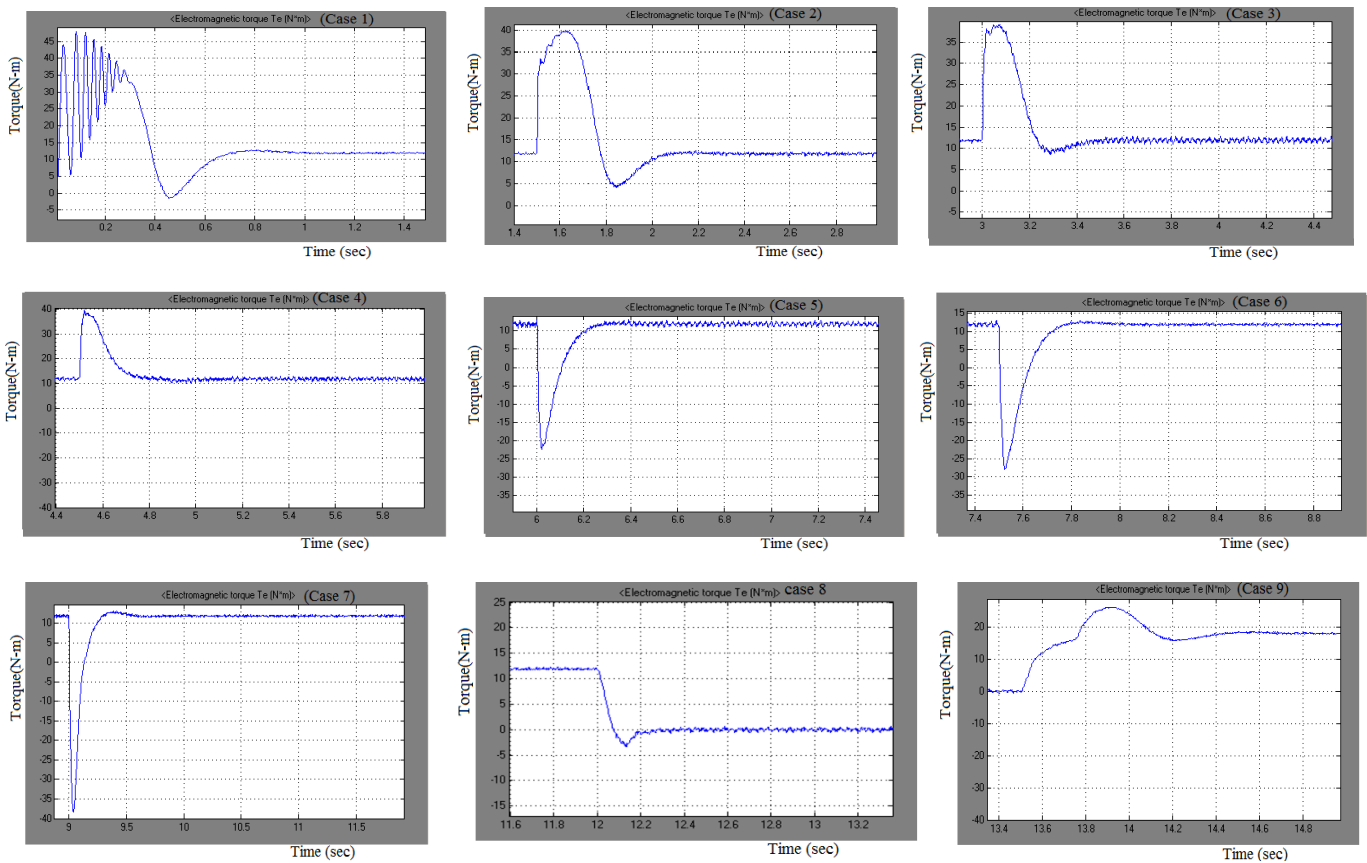


Fig.8 - Rotor speed responses of the drive system for entire cases



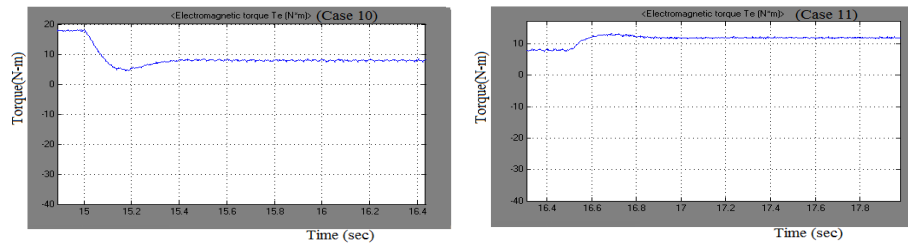


Fig. 9- Torque responses of the drive system for entire cases

Case-1: Starting (0 to 500 rpm)

Initially the motor is at stand still. A step speed command of rated value (500rpm) from standstill is given to the drive system. PI speed controller sets the rotor speed to reference speed (500 rpm) in 1.23 sec as shown in Fig. 8 (case 1). The electromagnetic torque corresponding to the reference speed (500 rpm) and the rated load torque (11.9 N-m) is found to be 11.87 N-m as shown in Fig 9 (case 1).

Case-2: Speed acceleration (500rpm to 1000 rpm)

The reference speed command to the drive system running at (500 rpm) is changed to (1000 rpm) instantly after 1.5 seconds and as a result the motor starts accelerating and settles to reference speed (1000 rpm) in 0.62 seconds as shown in Fig. 8(case 2). The electromagnetic torque corresponding to the reference speed (1000 rpm) and rated load torque (11.9 N-m) command is realized 12.06 N-m as shown in Fig.9(case 2)

Case-3: Speed acceleration (1000rpm to 1400 rpm)

The reference speed command to the drive system running at (1000 rpm) is changed to (1400 rpm) instantly after 3 seconds the motor starts accelerating and the motor settles to reference speed (1400 rpm) in 0.51 seconds as shown in Fig.8(case 3). The steady-state value of the electromagnetic torque corresponding to the reference speed (1400 rpm) and rated load torque (11.9 N-m) command is found to be 11.98 N-m as shown in Fig.9 (case 3).

Case-4: Speed acceleration (1400rpm to 1725 rpm)

The reference speed command to the drive system running at 1400 rpm is changed to 1725 rpm instantly after 4.5 seconds the motor starts accelerating and the motor settles to the reference speed (1725 rpm) in 0.72 seconds as shown in Fig.8(case 4). The steady-state value of the electromagnetic torque corresponding to the reference speed (1725 rpm) and rated load torque (11.9 N-m) command is observed 12.42 N-m as shown in Fig.9 (case 4).

Case-5: Speed deceleration (1725 rpm to 1400rpm)

The reference speed command to the drive system running at 1725 rpm is changed to 1400 rpm instantly after 6 seconds the motor starts decelerating and settles to reference speed (1400 rpm) in 0.39 seconds as shown in Fig.8 (case 5). The electromagnetic torque corresponding to the reference speed (1400 rpm) and rated load torque (11.9 N-m) command is found to be 11.46 N-m as shown in Fig.9 (case 5).

Case-6: Speed deceleration (1400 rpm to 1000 rpm)

The reference speed command to the drive system running at 1400 rpm is changed to 1000 rpm instantly after 7.5 seconds the motor starts decelerating and settles to the reference speed (1000 rpm) in 0.42 seconds as shown in Fig. (case 6). The steady-state value electromagnetic torque corresponding to the reference speed command (1000 rpm) and rated torque (11.9 N-m) is observed 11.82 N-m as shown in Fig.9 (case 6).

Case-7: Speed deceleration (1000 rpm to 500 rpm)

The reference speed command to the drive system running at 1000 rpm is changed to 500 rpm instantly after 9 seconds the motor starts decelerating and settles to reference speed command of 500 rpm in 0.74 seconds shown in Fig. 8 (case 7). The steady-state value of the electromagnetic torque corresponding to the reference speed (500 rpm) and rated load torque (11.9 N-m) command is realized 11.8 N-m as shown in Fig..7(case 7)

Case-8: Decrease in load torque (11.9 N-m to 0 N-m)

The rated load torque (11.9 N-m) of the motor running at 500 rpm is now reduced from 11.9 N-m to 0 N-m immediately after 13.5 seconds. The rotor speed tends to increase and it settles to 521 rpm in 0.36 seconds as depicted in Fig.8 (case 8). The steady-state value of the electromagnetic torque corresponding to the reference speed (500 rpm) and reference load torque (0 N-m) is realized 0.063 N-m as shown in Fig.9 (case 8).

Table I. Performance Of The Drive For Each Alteration In Reference Speed Keeping Load Torque $T_l=11.9$ N-m

Case	Speed step		Load torque (N-m)	Rotor speed (rpm)	Speed over shoot / under shoot	Drive running time (s)	Drive settling time (s)
	from	To					
1	0	500	11.87	500	35.2	1.5	1.23
2	500	1000	12.06	1000	11.2	3.0	0.62
3	1000	1400	11.98	1400	2.7	4.5	0.51
4	1400	1725	12.42	1725	-	6.0	0.72
5	1725	1400	11.46	1400	-	7.5	0.39
6	1400	1000	11.82	1000	-	9.0	0.42
7	1000	500	11.8	500	-	10.5	0.74

Table II. Performance Of The Drive For Each Alteration In Load Torque Keeping Rotor Speed = 500 rpm

Case	Torque step		Load torque (N-m)	Rotor speed (rpm)	Speed over shoot / under shoot	Drive running time (s)	Drive settling time (s)
	from	to					
8	11.9	0	0.063	521	9.8	13.5	0.36
9	0	18	18.34	500	26.2	15.0	1.12
10	18	8	7.735	500	9.8	16.5	0.34
11	8	11.9	11.95	500	-	18.0	0.29

Case-9: Increase in load torque (0 N-m to 18 N-m)

The load torque of the motor running at 500 rpm is now increased from 0 N-m to 18 N-m immediately after 15 seconds the rotor speed tends to decrease but it again settles to 500 rpm in 1.12 seconds as shown in Fig.8 (case 9). It can be observed from Fig.28 that the electromagnetic torque corresponding to reference speed (500) rpm and reference load torque (18 N-m) is found to be 18.34 N-m as shown in Fig.9 (case 9).

Case-10: Decrease in load torque (18 N-m to 8 N-m)

The load torque of the motor running at 500 rpm is now reduced from 18 N-m to 8 N-m immediately after 16.5 seconds the rotor speed tends to increase but it again settles to 500 rpm in 0.34 seconds as depicted in Fig.8 (case 10). The steady-state value of the electromagnetic torque corresponding to reference speed (500) rpm and reference load torque (8 N-m) is found to be 7.735 N-m as shown in Fig.9 (case 10).

Case-11: Increase in load torque (8 N-m to 11.9 N-m)

The load torque of the motor running at 500 rpm is now increased from 8 N-m to 11.9 N-m immediately after 18 seconds the rotor speed tends to decrease but it again settles to 500 rpm in 0.29 seconds as shown in Fig.8 (case 11). It can be observed from Fig.28 that the electromagnetic torque corresponding to reference speed (500) rpm and reference load torque (11.9 N-m) is realized to (11.95 N-m) as shown in fig.9 (case 11).

V. CONCLUSION

In this paper an induction motor drive based on the parallel assembly of the LCI and the VSI has been discussed. The performance of the Load Commutated Inverter fed induction motor drive has been investigated through the MATLAB/Simulation for the different alteration in reference speed and load torque. Simulation results shows that the presented drive system provides the more satisfactory results than the conventional CSI and VSI.



International Journal of Recent Development in Engineering and Technology
Website: www.ijrdet.com (ISSN 2347-6435(Online) Volume 2, Issue 2, February 2014)

VI. APPENDIX

Name plate ratings of induction motor
3-hp, three-phase, 220 V, 60Hz, 4-pole, 1725 r.p.m.
Star connected.

Induction motor parameters

$$R_s = 0.435 \Omega, R_r = 0.816 \Omega, L_s = 0.004 \text{ H}$$
$$L_r = 0.004 \text{ H}, L_m = 0.06931 \text{ H}, J = 0.089 \text{ Kg}\cdot\text{m}^2.$$

VII. REFERENCES

- [1] Sangshin Kwak and Hamid A. Toliyat "A Hybrid Converter System for High-Performance Large Induction Motor Drives" IEEE transactions on energy conversion, vol. 20, no. 3, pp.504-511, September 2005.
- [2] Andrzej M. Trzynadlowski and Niculina Patriciu "A Hybrid, Current-Source/Voltage-Source Power Inverter Circuit" IEEE transactions on power electronics, vol. 16, no. 6, pp.866-871, november 2001.
- [3] J. R. Espinoza and G. Joos, "A current-source-inverter-fed induction motor drive system with reduced losses," IEEE Trans. Ind. Appl., vol.34, no. 4, pp. 796– 805, Jul./Aug.1998.
- [4] S. D. Umans and H. L. Hess, "Modeling and analysis of the waltz three phase induction motor configuration," IEEE Trans. Power App. Syst., vol. PAS-102, no. 9, pp. 2912–2921, Sep. 1983.
- [5] H. L. Hess, D. M. Divan, and Y. Xue, "Modulation strategies for a new SCR-based induction motor drive systems with a wide speed ranges," IEEE Trans. Ind. Appl., vol. 30, no. 6, pp. 1648–1655, Nov./Dec. 1994.
- [6] H. Mok, S. K. Sul, and M. H. Park, "A load commutated inverter-fed induction motor drive system using a novel dc-side commutation circuit," IEEE Trans. Ind. Appl., vol. 30, no. 3, pp. 736–745, May/Jun. 1994.
- [7] B. Singh, K. B. Naik, and A. K. Goel, "Steady state of an inverter-fed induction motor employing natural Commutation," IEEE Trans. Power Electron., vol. 5, no. 1, pp. 117–123, Jan. 1990.
- [8] A. Toliyat, N. Sultana, D. S. Shet, and J. C. Moreira, "Brushless permanent magnet (BPM) motor drive system using load-commutated inverter," IEEE Trans. Power Electron., vol. 14, no. 5, pp. 831–837, Sep.1999.
- [9] S. Nishikata and T. Kataoka, "Dynamic control of a self-controlled synchronous motor drive system," IEEE Trans. Ind. Appl., vol. IA-20, no.3, pp. 598–604, May/Jun. 1984.